Resistive tearing growth rate modification by equilibrium flow

J. De Jonghe† and R. Keppens

Centre for mathematical Plasma-Astrophysics, KU Leuven, Belgium

†jordi.dejonghe@kuleuven.be

KU LEUVEN

erc PROMINENT

Introduction

- *Motivation.* Resistive tearing instability can trigger magnetic reconnection. This may lead to eruptive events like solar flares and disruption of plasma confinement in tokamak devices.
- *Observation.* Many physical plasmas are subject to some background flow. This flow affects the tearing mode growth rate.
- *Research.* Study of 2 magnetic field configurations (a rotating magnetic field of fixed size and a Harris sheet) paired with different background velocity profiles, explored parametrically with the (open-source) linear 1D magnetohydrodynamic (MHD) spectroscopy code *Legolas* [1, 2].

Magnetohydrodynamic spectroscopy with Legolas

- *Input.* 1D stratified plasma in Cartesian or cylindrical geometry.
- *Output.* Eigenmodes and corresponding eigenfunctions of the linearised MHD equations (after 3D Fourier analysis)

$$\frac{\partial \rho}{\partial t} = -\nabla\cdot(\rho\boldsymbol{v}), \tag{1}$$

$$\rho\frac{\partial \boldsymbol{v}}{\partial t} = -\nabla p - \rho\boldsymbol{v}\cdot\nabla\boldsymbol{v} + \boldsymbol{J}\times\boldsymbol{B} + \rho\boldsymbol{g} + \mu\left[\nabla^2\boldsymbol{v} + \frac{1}{3}\nabla(\nabla\cdot\boldsymbol{v})\right], \tag{2}$$

$$\rho\frac{\partial T}{\partial t} = -\rho\boldsymbol{v}\cdot\nabla T - (\gamma-1)p\nabla\cdot\boldsymbol{v} - (\gamma-1)\rho\mathscr{L} + (\gamma-1)\nabla\cdot(\boldsymbol{\kappa}\cdot\nabla T) + (\gamma-1)\eta\boldsymbol{J}^2 + (\gamma-1)\mu\left|\nabla\boldsymbol{v}\right|^2, \tag{3}$$

$$\frac{\partial \boldsymbol{B}}{\partial t} = \nabla\times(\boldsymbol{v}\times\boldsymbol{B}) - \nabla\times(\eta\boldsymbol{J}) - \nabla\times\left[\frac{\eta_{\mathrm{H}}}{\rho}(\boldsymbol{J}\times\boldsymbol{B} - \nabla p_{\mathrm{e}}) + \frac{\eta_{\mathrm{e}}}{\rho}\frac{\partial \boldsymbol{J}}{\partial t}\right]. \tag{4}$$

Magnetic field rotation

- *Geometry.* Cartesian slab [-0.5, 0.5].
- *Equilibrium configuration.* Constant density and temperature, rotating magnetic field, and linear velocity profile

$$\rho_0(x) = \rho_0^{(c)}, \qquad \boldsymbol{B}_0(x) = \sin(\alpha x)\,\hat{\mathbf{e}}_y + \cos(\alpha x)\,\hat{\mathbf{e}}_z,$$
$$T_0(x) = \frac{1}{2}\beta\boldsymbol{B}_0^2, \qquad \boldsymbol{v}_0(x) = v_{02}^{(c)}\,x\,\hat{\mathbf{e}}_y.$$

- *Specifics.*
  - Wavevector parallel to the velocity.
  - Magnetic field rotation between half a rotation and a full rotation ($\pi < \alpha < 2\pi$).

Velocity variation

- *Fixed parameters.*

$$\boldsymbol{k} = 1.5\,\hat{\mathbf{e}}_y, \quad \rho_0^{(c)} = 1, \quad \alpha = 4.73884, \quad \eta = 10^{-4}$$

(Note: we only consider sub-Alfvénic speeds.)

- *Varied parameters.* $v_{02}^{(c)}$, β
- *Observations.*
  - Both stabilising and destabilising.
  - β-independent dropoff.

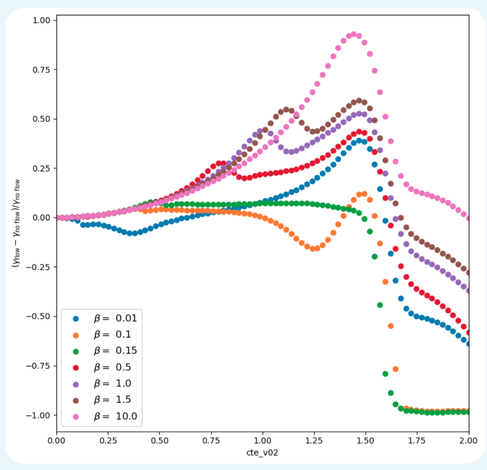

FIGURE 1: Relative tearing growth rate as a function of the velocity gradient for different β-values.

Density variation

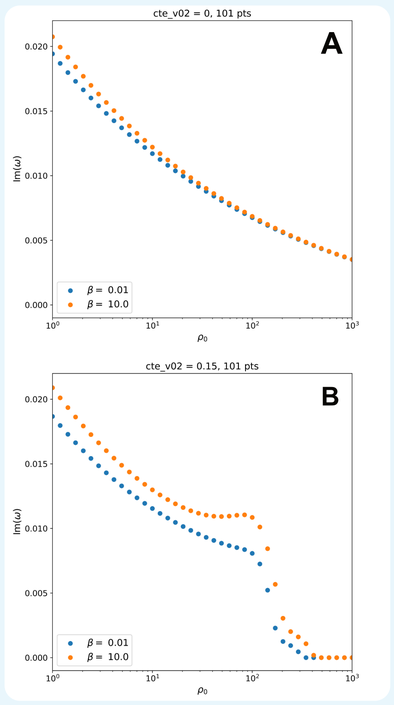

- *Fixed parameters.*

$$\boldsymbol{k} = 1.5\,\hat{\mathbf{e}}_y, \quad v_{02}^{(c)} = 0.15, \quad \alpha = 4.73884, \quad \eta = 10^{-4}$$

- *Varied parameters.* $\rho_0^{(c)}$, β
- *Observations.*
  - Growth rate decreases with increasing density.
  - The presence of a background flow introduces a new density dependence in the growth rate where the tearing mode is quickly and fully damped above a threshold density.
    1. Small density: largely unaltered
    2. Intermediate density: strong damping
    3. Large density: fully damped

  (Note: for both depicted cases, the plasma-β is much larger than 1 at the point of strong damping.)

FIGURE 2: Comparison of density variation in (A) the absence of flow and (B) presence of flow.

Resistivity variation

- *Fixed parameters.*

$$\boldsymbol{k} = 1.5\,\hat{\mathbf{e}}_y, \quad \rho_0^{(c)} = 1, \quad \alpha = 4.73884, \quad \beta = 0.15$$

- *Varied parameters.* η, $v_{02}^{(c)}$
- *Observations.*
  - Whether a background flow of given speed exerts a stabilising or destabilising influence on the tearing mode depends strongly on the resistivity.

FIGURE 3: Relative tearing growth rate as a function of the resistivity for various flow speeds.

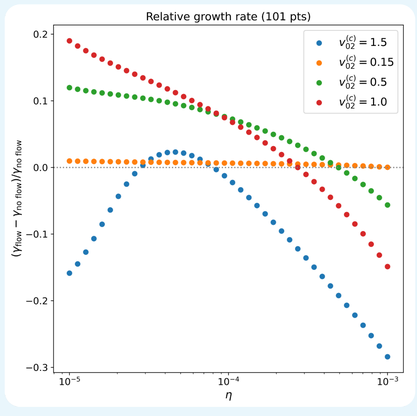

Harris sheet

- *Geometry.* Cartesian slab [-15, 15].
- *Equilibrium configuration.* Constant density, hyperbolic tangent profile for both magnetic field and velocity, and temperature satisfying the force-balance equation

$$\rho_0(x) = \rho_0^{(c)}, \qquad \boldsymbol{B}_0(x) = B_0^{(c)}\tanh\left(\frac{x}{a_{\boldsymbol{B}}}\right)\hat{\mathbf{e}}_y,$$
$$T_0(x) = \frac{\left(B_0^{(c)}\right)^2 - \boldsymbol{B}_0^2}{2\rho_0}, \qquad \boldsymbol{v}_0(x) = v_{02}^{(c)}\tanh\left(\frac{x}{a_{\boldsymbol{v}}}\right)\hat{\mathbf{e}}_y.$$

- *Specifics.*
  - Wavevector parallel to the velocity.

Wavenumber variation

- *Fixed parameters.*

$$\rho_0^{(c)} = B_0^{(c)} = a_{\boldsymbol{B}} = a_{\boldsymbol{v}} = 1, \quad \eta = 10^{-3}$$

- *Varied parameters.* k, $v_{02}^{(c)}$
- *Observations.*
  - Both stabilising and destabilising.
  - Peak apparently around fixed wavenumber.
  - Transition from stabilising to destabilising k value is velocity dependent.

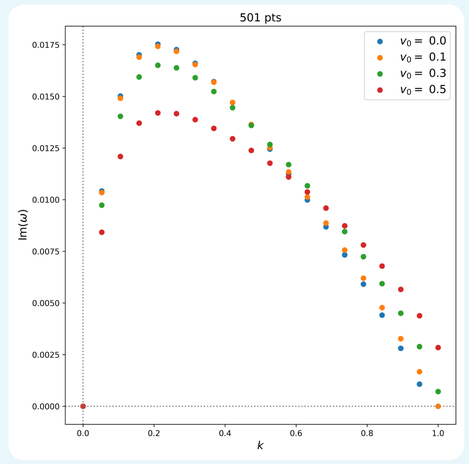

FIGURE 4: Tearing growth rate as a function of the wavenumber k for different maximal velocities.

Velocity profile parameter variation

- *Fixed parameters.*

$$k = 0.5, \quad \rho_0^{(c)} = B_0^{(c)} = a_{\boldsymbol{B}} = 1, \quad \eta = 10^{-4}$$

- *Varied parameters.* $v_{02}^{(c)}$, $a_{\boldsymbol{v}}$
- *Observations.*
  - Both stabilising and destabilising.
  - If the velocity transition width is larger than the Harris sheet width, the flow works mostly destabilising.
  - The transition from destabilising to stabilising influence depends on both the velocity transition width and the maximal speed.
  - When the velocity transition width is smaller than the Harris sheet width and the maximal speed approaches the Alfvén speed, the Kelvin-Helmholtz instability becomes the most unstable mode in the system (top right corner of figure 5). It is an order of magnitude larger than the tearing mode.

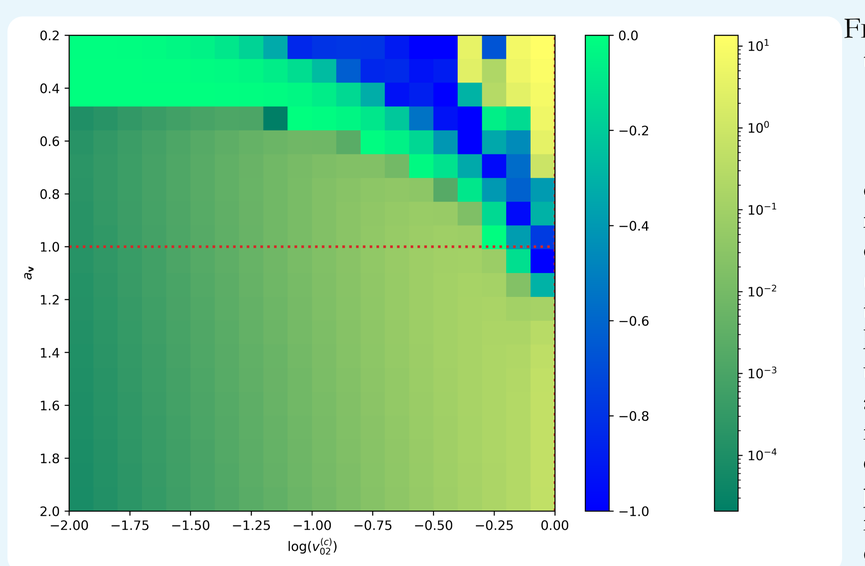

FIGURE 5: Visualisation of the relative growth rate

$$\frac{\mathrm{Im}(\omega) - \mathrm{Im}(\omega_{\text{no flow}})}{\mathrm{Im}(\omega_{\text{no flow}})}$$

of the most unstable mode for combinations of maximal flow speed (x-axis) and flow transition width (y-axis). Different colour maps are used for damped (< 0) and destabilised (> 0) regions. Red dotted lines denote the equivalent **B**-parameters. (20x20 *Legolas* runs of 501 grid points each.)

Acknowledgements

This study is supported by funding from the European Research Council (ERC) under the European Union Horizon 2020 Research and Innovation Program, grant agreement no. 833251 PROMINENT ERC-ADG 2018. More information about the project can be found on the website.

References

[1] Claes, N., De Jonghe, J. & Keppens, R. 2020 Legolas: A modern tool for magnetohydrodynamic spectroscopy. *Astrophys. J., Suppl. Ser.* **245** (2), 45.

[2] De Jonghe, J., Claes, N. & Keppens, R. 2022 Legolas: Magnetohydrodynamic spectroscopy with viscosity and Hall current. *J. Plasma Phys.* (in press).